INTERNATIONAL JOURNAL FOR NUMERICAL METHODS IN FLUIDS, VOL. 8, 1439–1458 (1988)

ACCURACY OF A DETERMINISTIC PARTICLE METHOD FOR NAVIER–STOKES EQUATIONS

J. P. CHOQUIN

CMAP, Ecole Polytechnique, 91128 Palaiseau, France

AND

B. LUCQUIN-DESREUX

ONERA, 29 Av de la Division Leclerc, 92320 Chatillon, France

SUMMARY

The accuracy of a deterministic particle method in approximating the solution of the Navier–Stokes equations is investigated. The convective part is solved using a classical vortex method for inviscid fluids, and an iterative procedure is added to improve the interpolation of the vorticity function. In our examples the vorticity is radially symmetric. For a regular initial data, a discrete quadratic error on the velocity and the vorticity is considered. Otherwise, for a singular initial data, the exact and computed angular moments of the vorticity are compared.

KEY WORDS Cut-off function Particle approximation Viscous flow Vortex method

INTRODUCTION

The two-dimensional flow of an incompressible viscous fluid is described by the Navier–Stokes equations. We use a velocity–vorticity formulation:

$$\partial\omega/\partial t + (U\cdot\nabla)\omega - \nu\Delta\omega = 0, \qquad \omega(z,0) = \omega_0, \tag{1}$$

$$\operatorname{div}(U) = 0, \qquad \operatorname{rot}(U) = \omega, \qquad U \to 0 \quad \text{when } \|z\| \to \infty, \tag{2}$$

where $U(z,t)$ is the velocity field ($z=(x,y)\in\mathbb{R}^2$, $t>0$), ω is the vorticity, ν is the kinematic viscosity and z represents the spatial co-ordinates.

When classical methods (finite element or finite difference methods) are used to simulate this flow at high Reynolds number, a fine mesh is required to avoid introducing grid-scale disssipation and dispersion errors. To overcome these difficulties, Chorin[1] has proposed a grid-free algorithm which is a fractional step method. The vorticity field is discretized through vortex-carrying particles. At each time step the convective part of the Navier–Stokes equations is solved by following these particles throughout the fluid (vortex method). The diffusion part is treated by superimposing a Gaussian random walk on the velocity of the particles. This method has been successfully applied to many cases.[1–3]

Recently, another way to treat the viscous term was developed by Cottet and Gallic[4] and Huberson.[5] This approximation uses an exact similarity solution of the heat equation for an initial condition restricted to a single source and an infinite domain. Up to now, applications of

0271–2091/88/111439–20$10.00

Received 14 May 1987
Revised 28 January 1988

this method include mixing layers,[6] aerodynamic calculations[5] and comparisons with exact solutions.[7]

In a recent work by Mas-Gallic and Raviart,[8] the conservative version of this method has been found to derive from a more general methodology for computing the solution of symmetric hyperbolic systems. This leads to a new extended class of numerical schemes which can be interpreted as a 'generalized finite difference formulation'. The proposal of this paper is to apply this new deterministic particle approximation of the diffusion in the more general case of the Navier–Stokes equations. In order to investigate the accuracy of such an algorithm, we shall consider numerical examples for which an exact analytical solution is known; this will permit a precise computation of the error made by replacing the exact solution by its numerical approximation. Improvements, in comparison with the previous random walk proposed by Chorin, will be shown up as well.

The paper is divided into three parts. The first section presents the general method, describing in particular its two main new points which are: first, the particle approximation of the Laplacian operator, and secondly, an efficient numerical algorithm for the interpolation of the vorticity function. The second section is devoted to computational tests. Two examples are considered. They are of radial symmetry, only in order to obtain an exact analytical solution, and of various regularity, in order to see if the method can work with singular initial data. Results are then presented and discussed in the third section.

THE NUMERICAL METHOD

The main idea of vortex methods is to follow fluid elements, called vortex particles, in a Lagrangian description of the flow. Because of the incompressibility condition, the volume of each particle remains constant in time. It is thus sufficient to follow the evolution of one point which represents the particle; this point is mathematically represented by a Dirac measure.

We introduce a square grid of uniform mesh size h. Each cell P_j is centred at a grid point z_j. The initial vorticity distribution is approximated by a linear combination of Dirac measures:

$$\omega_0^h(z) = \sum_j h^2 w_j \delta(z - z_j), \qquad w_j = \omega_0(z_j), \tag{3}$$

where δ denotes the Dirac measure.

The Lagrangian representation of the flow allows a direct integration of the convective part of equation (1). The method used here remains similar on that point to the classical vortex method which has been detailed in many other works (e.g. see Reference 9). The approximate solution $\omega^h(z, t)$ of $\omega(x, t)$ is:

$$\omega^h(z, t) = \sum_j h^2 w_j(t) \delta(z - z_j(t)), \tag{4}$$

where $z_j(t)$ is the location of the particle j at time t and $w_j(t)$ is an approximation of $\omega(z_j(t), t)$.

Given a sufficiently smooth approximation U^h of the velocity field, the particle path $z_j(t)$ is the solution of the differential system:

$$\mathrm{d}z_j(t)/\mathrm{d}t = U^h(z_j(t), t) \qquad z_j(0) = z_j. \tag{5}$$

Let us consider now the diffusion term in (1). It is evaluated by generalized finite differences. For this computation a sufficiently smooth approximation of the vorticity field is required. In order to obtain this approximation, we introduce (in non-dimensional variables) $\zeta_\varepsilon(z) = (1/\varepsilon^2)\zeta(z/\varepsilon)$, a smooth approximation of the delta measure, ε being a scaling parameter[9] and ζ a radially

symmetric function. The value of $w_j(t)$ appearing in (4) is obtained by solving the following differential system:

$$dw_j(t)/dt = F(w_j(t)), \qquad w_j(0) = w_j, \tag{6}$$

$$F(w_j(t)) = (2v)h^2 \sum_k (w_k(t) - w_j(t)) \frac{D\zeta_\varepsilon(z_j(t) - z_k(t))(z_k(t) - z_j(t))}{\| z_j(t) - z_k(t) \|^2}. \tag{7}$$

We can briefly explain the consistency of the algorithm by showing how $v\Delta\omega(z_j(t), t)$ is approximated by $F(w_j(t))$. Within a quadrature error, we have to estimate the difference:

$$E(z, t) = \Delta\omega(z, t) - 2 \int_{\mathbb{R}^2} (\omega(z', t) - \omega(z, t)) \frac{D\zeta_\varepsilon(z - z') \cdot (z' - z)}{\| z - z' \|^2} dz'.$$

By Taylor's formula with integral remainder we have

$$E(z, t) = \Delta\omega(z, t) - 2 \sum_{q=1}^{k+1} 1/q! \sum_{|\alpha| = k} \frac{\partial^\alpha \omega}{\partial z^\alpha}(z, t) I_\alpha + R(z, t),$$

where k is the order of approximation. The main part of the demonstration is the following consistency result: $I_\alpha = 1$ if $\alpha = (2, 0)$ or $(0, 2)$ and $I_\alpha = 0$ otherwise, so that $E(z, t) = R(z, t)$. The proof, detailed in Reference 8, is briefly recalled in the Appendix. We then have $|E(z, t)| \leqslant c\varepsilon^k$. If we consider a quadrature formula, the difference between $\Delta\omega(z, t)$ and $(1/v)F(w_j(t))$ is of order $\varepsilon^k + h^m/\varepsilon^{m+1}$. To complete the algorithm, the velocity U^h has to be related to the vorticity ω^h. In the case of the continuous problem the velocity is related to the vorticity by a convolution with a singular kernel K according to the Biot–Savart law:

$$U(z, t) = K^* \omega(.\,, t)(z), \quad \text{where } K(z) = \frac{1}{2\pi |z|^2}(-y, x). \tag{8}$$

In the particle method the kernel K is regularized by use of a cut-off function. We use the same function ζ_ε that was previously introduced in (7). The approximate velocity U^h is then given by

$$U^h(z, t) = K_\varepsilon^* \omega^h(.\,, t)(z), \quad \text{where } K_\varepsilon = K^* \zeta_\varepsilon. \tag{9}$$

Notice that considering a Euler explicit scheme with time step Δt for the integration of (5) and a Gaussian function of strength $\varepsilon = (4\Delta t R^{-1})^{0.5}$ for ζ_ε, the weights given by the conservative form of the splitting algorithm[6] and the previous method are the same. The fractional step method proposed by Cottet–Gallic and Huberson can be therefore considered as a particular case of the particle algorithm described above.

For the case of an inviscid fluid theoretical results of convergence have been obtained by many authors.[9, 10] In that case the weight of the particle remains constant in time. Consider smooth initial data and a sufficiently smooth function ζ_ε which approximates δ to order k;[9] the error estimate on the velocity in L^∞ *is* $\varepsilon^k + h^m/\varepsilon^{m-1}$, where m is related to the regularity of ζ.

The theoretical analysis of the method in the non-linear case has not yet been carried out except for the particular case of the splitting algorithm.[4] The error estimate on the velocity in L^p is in this case $(v\Delta t)^{1/2}$, with a stability condition $h^2 < Cv\Delta t$, which gives a relation between the number of particles and the Reynolds number.

The velocity computation which is necessary for the determination of the particle paths can be done, as described in (9), by use of the regularization of the kernel K. The velocity is thus

$$U^h(z, t) = \sum_j h^2 w_j(t) K_\varepsilon(z - z_j(t)). \tag{10}$$

The velocity can also be obtained by a regularization of the vorticity:

$$\omega_\varepsilon^h(z,t) = \sum_j h^2 w_j(t)\zeta_\varepsilon(z - z_j(t)). \tag{11}$$

Then

$$U^h(z,t) = K * \omega_\varepsilon^h(.,t)(z).$$

In the case of an inviscid flow the weight $w_j(t)$ of the particle j is constant:

$$w_j(t) = w_j = \omega_0(z_j).$$

The main source of error is related to the quadrature formulae contained in (10) and (11). Possible improvements have been proposed, such as rezoning,[11] more accurate integration rules[12] or improvement of the interpolation (11) of the vorticity function.[13] The last one is used here; it is based on a 'scattered data interpolation'.[14] The idea is to choose coefficients γ_j so that

$$w_j = \sum_k h^2 \gamma_k \zeta_\varepsilon(z_j(t) - z_k(t)) \tag{12}$$

or

$$A\gamma = w, \qquad \gamma = (\gamma_j), \qquad w = (w_j); \qquad A_{j,k} = h^2 \zeta_\varepsilon(z_j(t) - z_k(t)).$$

This is done by an iterative procedure. Starting with $\gamma^0 = w$, then

$$\gamma^{n+1} = \gamma^n + (w - A\gamma^n). \tag{13}$$

The coefficients γ_j^n, obtained by n internal iterations, permit a new computation U_h of the velocity:

$$U_h(z,t) = \sum_j h^2 \gamma_j^n K_\varepsilon(z - z_j(t)). \tag{14}$$

For the determination of the particle trajectories the approximate velocity U^h defined by (10) is thus replaced by U_h.

Theoretical results have recently been obtained in the case of the Euler equations.[13] Setting $\varepsilon = Ch^q$, $\frac{1}{4} \leqslant q \leqslant \frac{1}{2}$, and using (13) to compute the velocity, the velocity fields converge in L^p norm to $O(\varepsilon^{kn})$. In the case of the present algorithm we decided to use this procedure of internal iterations at each time step.

From now on we suppress the index ε and we call ω_h the computed value of the vorticity,

$$\omega_h(z,t) = \sum_j h^2 \gamma_j(t)\zeta_\varepsilon(z - z_j(t)), \tag{15}$$

so that $U_h = K * \omega_h$.

THE MODEL PROBLEM

As explained in the Introduction, our test problem consists of solving equations (1) and (2) with a radially symmetric initial condition. It follows that the vorticity equation (1) reduces to

$$\partial\omega/\partial t - \nu\Delta\omega = 0; \tag{16}$$

ω is a solution of the heat equation and can be written in the form

$$\omega(z,t) = \int E_\nu(z - z', t)\omega_0(z')\,dz', \tag{17}$$

where ω_0 is the initial distribution of vorticity and E_ν is the fundamental solution for the heat equation:

$$E_\nu(z,t)=\frac{1}{4\pi\nu t}\exp\left(-\frac{\|z\|^2}{4\nu t}\right). \tag{18}$$

However, let us emphasize that in the numerical simulation no particular advantage is taken of this radial symmetry: the complete convection–diffusion equation of the vorticity (1) is considered instead of the pure heat equation (16).

In order to determine the accuracy of the numerical method, we calculate the exact and numerical values of the velocity and vorticity fields at the particle locations and use a discrete norm to measure the error. Let us denote by U_e and ω_e the exact values of the velocity and vorticity fields and by U_h and ω_h the corresponding numerical values. Then the two relative errors considered here are

$$E_U(t)=\left(\sum_j (U_h(z_j(t),t)-U_e(z_j(t),t))^2/\sum_j U_e(z_j(t),t)^2\right)^{0.5}, \tag{19}$$

$$E_\omega(t)=\left(\sum_j (\omega_h(z_j(t),t)-\omega_e(z_j(t),t))^2/\sum_j \omega_e(z_j(t),t)^2\right)^{0.5}. \tag{20}$$

These two errors can be easily computed in the case where the exact velocity and vorticity have explicit expressions. However, when this is not possible, it is a common practice to compare the exact and computed values of an easily computable functional. As Milinazzo and Saffman did,[15] we choose the functional

$$M(t)=\int |z|^2\omega(z,t)\,dz \Big/ \int \omega(z,t)\,dz. \tag{21}$$

This functional satisfies the equation

$$M(t)=M(0)+4t\nu.$$

In the particle method M can be approximated by

$$M_h(t)=N_h(t)/D_h(t), \tag{22}$$

where

$$N_h(t)=\sum_j |z_j(t)|^2 h^2 \omega_h(z_j(t),t)$$

and

$$D_h(t)=\sum_k \Omega_k(t), \qquad \Omega_k(t)=h^2 w_k(t).$$

Then the error we measure is

$$E_M(t)=|M(t)-M_h(t)|/|M(t)|.$$

The first test case presented corresponds to initial data of the form:

$$\omega_0(z)=c\frac{1}{4\pi\nu t_1}\exp\left(-\frac{\|z\|^2}{4\nu t_1}\right)=cE_\nu(z,t_1),$$

where c is a constant,

$$\omega(z,t) = cE_\gamma(z, t+t_1),$$

$$U(z,t) = \frac{c}{2\pi\|z\|^2}\left[1-\exp\left(\frac{-1}{4\nu(t+t_1)}\|z\|^2.\right)\right]\begin{bmatrix}-y\\ x\end{bmatrix}.$$

In that case the vorticity and the velocity are $C^\infty(\mathbb{R}^2)$ and have unbounded support.

In the second test case a discontinuous vorticity distribution is chosen:

$$\omega_0 = \begin{cases}1, & \|z\| \leqslant 1,\\ 0, & \text{otherwise.}\end{cases}$$

Even in the case of the Euler equations there are no theoretical results of convergence for such kind of singular initial data. However, it would be of some interest to see if the method can work with such initial data.

NUMERICAL RESULTS

The computations are carried out in non-dimensional variables. Using the same notations for the dimensional and the non-dimensional variables and the same expressions as above, ν becomes equivalent to the inverse of the Reynolds number, and the characteristic length is implicitly defined by the expression of the initial vorticity. In the first test case the characteristic velocity U_0 is defined to be the root mean square value of the initial velocity, and the numerical value of c is adjusted for each Reynolds number so as to produce $U_0 = 1$.

For a fixed time interval $[0, T]$ the accuracy of the method depends on

(i) The choice of the regularization function ζ and the cut-off parameter $\varepsilon = h^p$
(ii) the number of particles n_q
(iii) the number of internal iterations n_γ of process (13).

In all our computations we use a function ζ which is an approximation of order three of the Dirac measure:[7]

$$\zeta(r) = \frac{2}{\pi}\frac{2-r^2}{(1+r^2)^4}. \tag{23}$$

We choose an Adams–Bashforth scheme of order two for the time discretization of equations (5) and (6) and we study the influence of the other parameters, $\varepsilon = h^p$, n_q and n_γ, and of the Reynolds number R.

First we present the results for the case:

$$\omega_0(z) = c\frac{1}{4\pi\nu t_1}\exp\left(-\frac{1}{4\nu t_1}\|z\|^2\right). \tag{24}$$

At time $t = 0$ the particles are equally distributed in the square $S = [-2,2]^2$. Setting

$$\eta(t) = \int_S \omega(z,t)\,dx \Big/ \int_{\mathbb{R}^2} \omega(z,t)\,dx,$$

t_1 is chosen so that $\eta(0)$ is greater than 0·9999, and we fixed $\Delta t = 0{\cdot}03$. Theoretical results[9] show that for the inviscid case the accuracy of the particle method increases as $p(\varepsilon = h^p)$ increases. However, this result has been observed only for a short interval of time.[16] We expect the same result for the viscous case. We find that this holds as shown in Figure 1, where results are presented for a

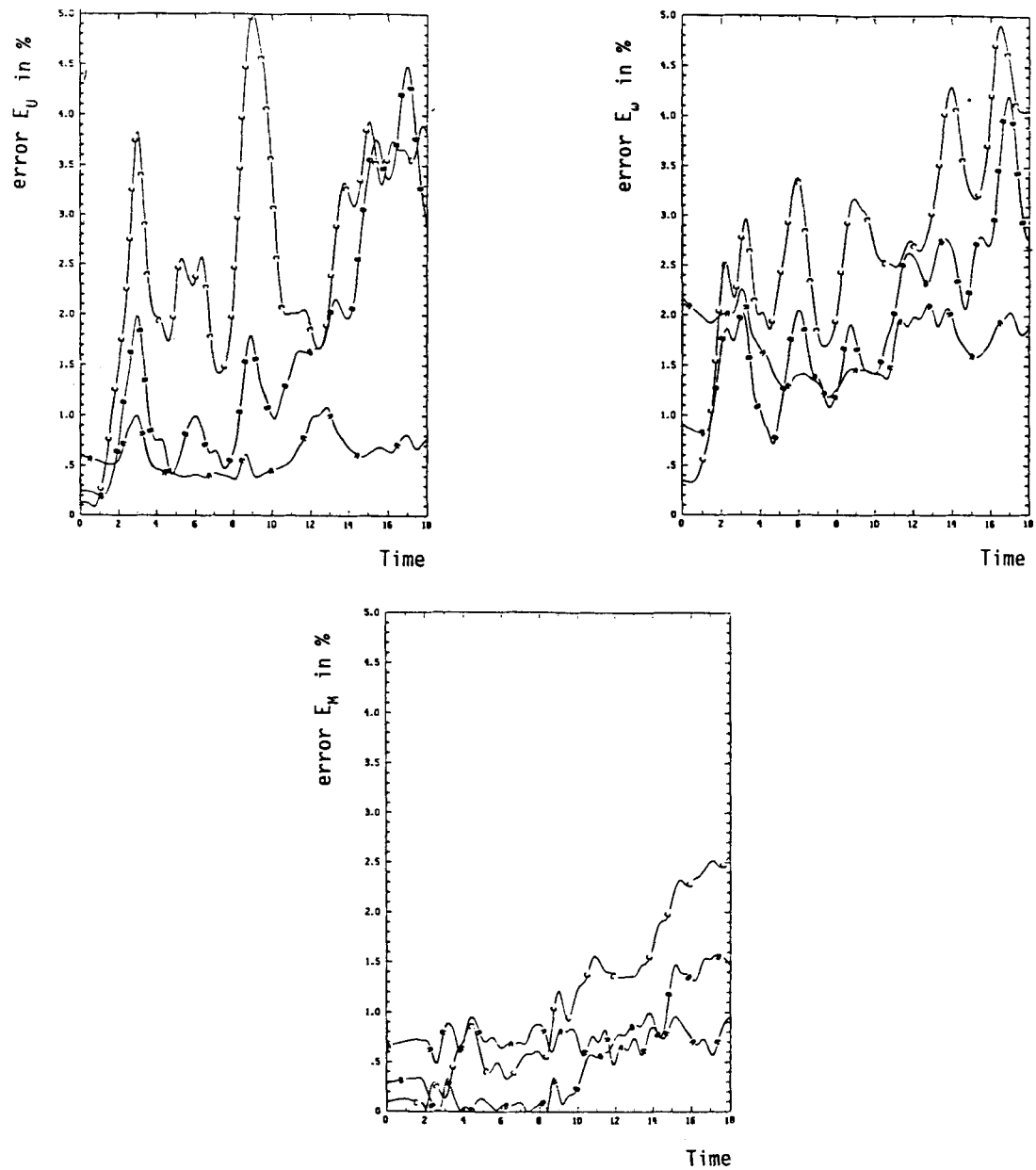

Figure 1. Influence of the cut-off parameter $\varepsilon = h^p$ for different values of p (A, 0·1; B, 0·2; C, 0·3); Navier–Stokes problem; regular case; $n_\gamma = 5$; $\Delta t = 0{\cdot}03$; 400 particles; $Re = 10^3$

Reynolds number of 1000, $n_q = 400$, $n_\gamma = 5$ and different values of p, $p = 0{\cdot}1, 0{\cdot}2, 0{\cdot}3$. After $t = 2$ we observe a sharp increase in the behaviour of the errors E_U and E_ω, and the better estimate is obtained for the largest value of ε which corresponds to $p = 0{\cdot}1$. As ε increases, the sharp increase of the errors is attenuated and a more uniform behaviour of the errors is observed in the time interval [0, 18]. A possible explanation is that the time discretization of the trajectories of the

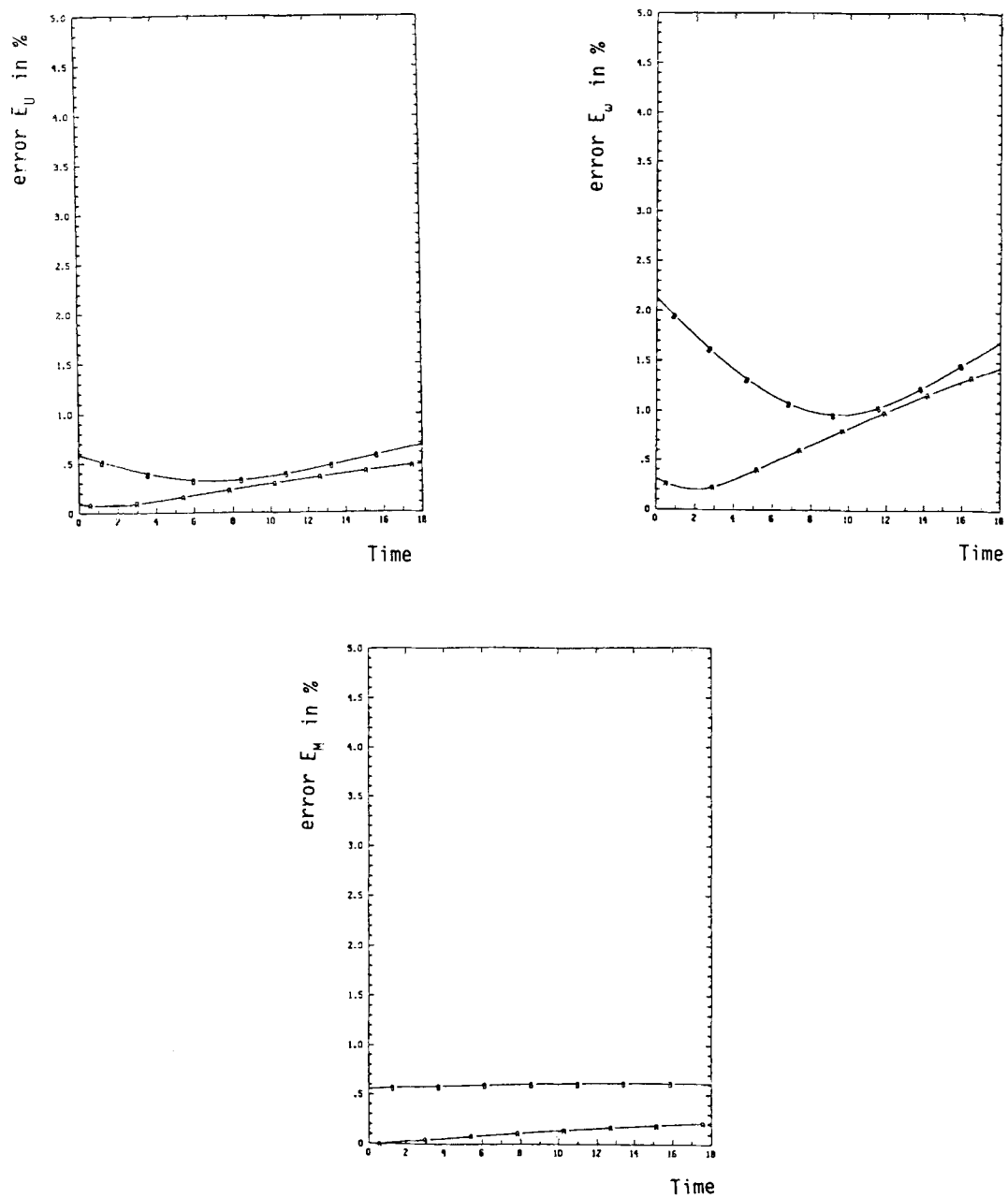

Figure 2. Influence of the cut-off parameter $\varepsilon = h^p$ for different values of p (A, 0·3; B, 0·1); Stokes problem; regular case; $n_y = 5$; $\Delta t = 0{\cdot}03$; 400 particles; $Re = 10^3$

particles induces an error in the discretized velocity. This error can be reduced by increasing the size of the cut-off parameter so that the integral is less singular. To try to confirm this hypothesis, we fixed the particle locations then solved only the Stokes problem. Figure 2 shows that the errors are smaller in that case when ε is smaller ($p = 0{\cdot}3$).

Table I. 400 particles; $Re = 10^3$; $n_\gamma = 5$; $\Delta t = 0{\cdot}03$; $\varepsilon = h^p$

p	0·08	0·1	0·2	0·3	0·33
$E_U(0)$	0·69	0·58	0·23	0·09	0·07
$E_U^{\max}$	1·0	1·08	4·48	5·0	7·0
$E_\omega^{\max}$	2·5	2·1	4·2	4·9	5·8
$E_M^{\max}$	1·3	0·95	1·6	2·5	3·8

We remark from Table I that, for the case of the Navier–Stokes equations, there is an optimal choice for ε which minimizes the three errors E_U, E_ω and E_M in the interval [0, 18]. This optimal choice for the numerical problem considered here is near $p = 0{\cdot}1$.

We look now at the errors E_U, E_ω and E_M as a function of n_γ for $n_q = 400$, $\varepsilon = h^{0{\cdot}3}$ and a Reynolds number of 1000. It is seen from Figure 3 that for $n_\gamma = 2$ or 5 the behaviour of the errors is very similar. At the beginning the errors increase sharply and tend to oscillate around a local maximum. In contrast to these two cases, we observe that for $n_\gamma = 0$ the increase in the errors is not so steep. However, in this last case the errors E_U and E_ω are important. They are not of the same order as for the two preceding cases, $n_\gamma = 2$ or 5. Thus the accuracy of the method is improved by the use of internal iterations. This is not as significant for the errors computed with the velocity E_U as for the errors based on the vorticity, E_ω and E_M. This has to be related with the fact that E_U, even for $n_\gamma = 0$, was not so bad at $t = 0$ compared with the value of E_ω at the same time.

The third example we present is the effect of varying the number n_q of particles. As n_q increases, h decreases, and we can see in Figure 4 the results for $n_\gamma = 5$, $\varepsilon = h^{0{\cdot}1}$, $n_q = 100$, 225, 400 and a Reynolds number of order 1000. This numerical example shows that the different values of n_q used do not allow us to confirm the theoretical results. The errors do not in fact decrease with h. However, we observe that the influence of n_q is more sensitive on the errors computed with the vorticity, E_ω and E_M.

In Figure 5 we present results for the same case as in Figure 1 but for a higher Reynolds number, $Re = 10000$. A comparison between Figures 1 and 5 shows that the errors are of the same order of magnitude and the better estimate is here obtained for $p = 0{\cdot}1$; although we find that for $p = 0{\cdot}2$ the results are better in the case $Re = 10000$ than for $Re = 1000$. In fact, for high Reynolds numbers the flow tends to be inviscid; for this case numerical results[16] show that p must be chosen larger than in the viscous case we consider here. Thus for a fixed number of particles we must increase p if we increase the Reynolds number.

We now consider the second test problem:

$$\omega_0(z) = 1 \quad \text{if } \|z\| \leqslant 1,$$

$$\omega_o(z) = 0 \quad \text{if } \|z\| > 1.$$

The effect of the diffusion will be an instantaneous smoothing of the vorticity. The initial distribution of particles is located in the square $[-R, R]^2$, where R is greater than 1. For this initial condition the integral (17) is very costly to compute, so we do not use the errors E_U and E_ω but only E_M. Let us point out that this quantity has been found to vary in the same way as the two other computed errors in the previous example.

It is seen from Figure 6 that the behaviour of the error E_M as a function of ε is similar at the beginning of the calculation to that previously observed (Figure 1): the best value of the error is obtained for the smallest value of ε. For $p = 0{\cdot}5$ or 0·6 the curves are similar but the error is a little bit lower in the case $p = 0{\cdot}5$. From Table II we find, as in the first test case, that there exists an optimal choice for ε which is near the value $p = 0{\cdot}5$.

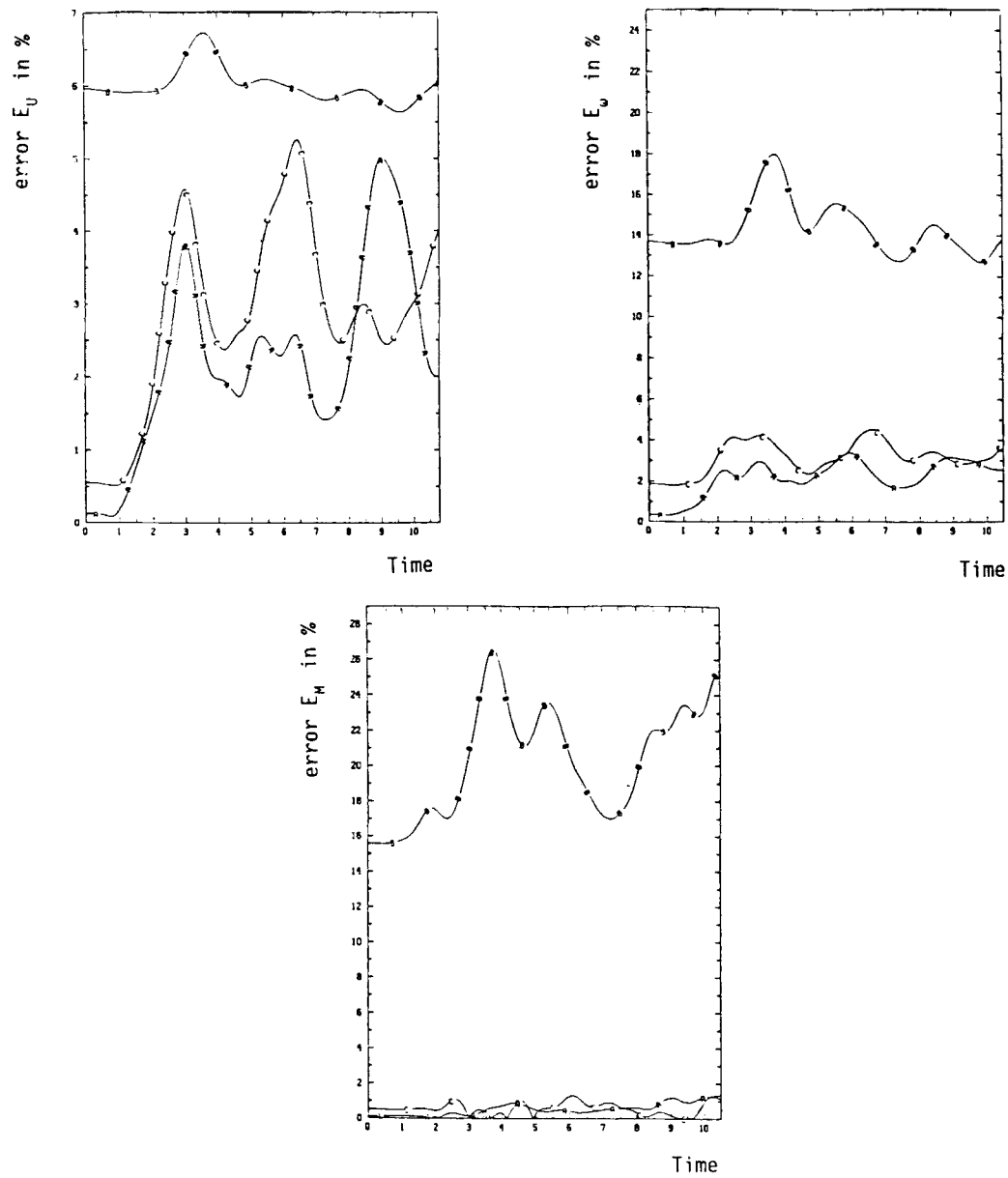

Figure 3. Influence of the number n_γ (A, 5; B, 0; C, 2) of internal iterations; Navier–Stokes problem; regular case; $\varepsilon = h^{0.3}$; $\Delta t = 0.03$; 400 particles; $Re = 10^3$

In Figure 7 we can see the influence of the parameter n_γ. As in the previous example (Figure 3), the behaviour of the error is very similar for $n_\gamma > 1$. The case $n_\gamma = 0$ gives large values of the error and has not been drawn in this figure.

We see in Figure 8 a large decrease in the error as a function of the number of particles (225 and 400 particles). However, it does not seem useful to increase this number over a certain value as it does not really improve the results (400 and 625 particles).

These examples show that the method works even with singular initial data.

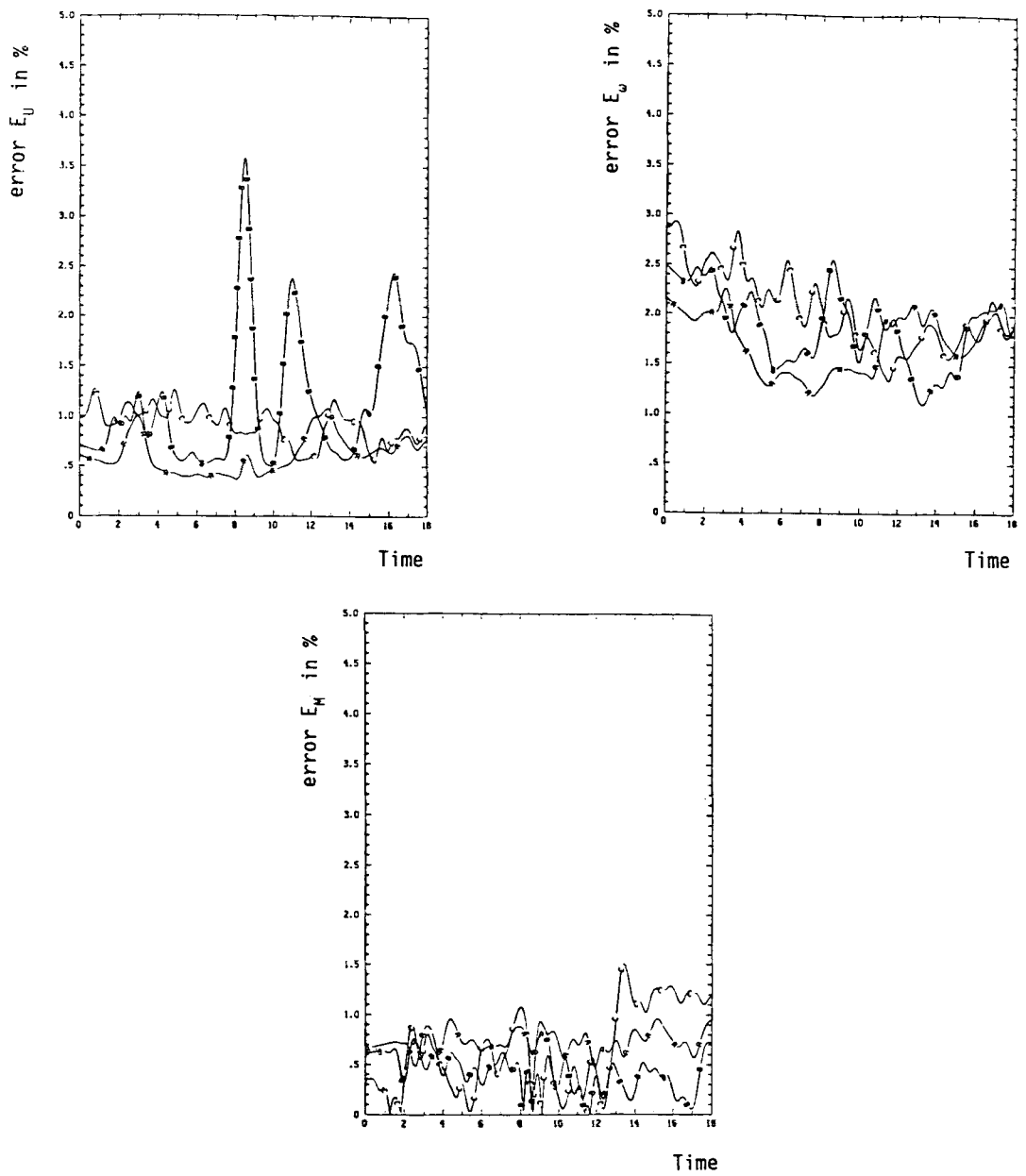

Figure 4. Influence of the number n_q (A, 400; B, 225; C, 100) of particles; Navier–Stokes problem; regular case; $\varepsilon = h^{0.1}$; $n_\gamma = 5$; $\Delta t = 0.03$; $Re = 10^3$

Finally, if we increase the Reynolds number, with a fixed number of particles ($n_q = 400$), we find that the error is more important at higher Reynolds number (Figure 9). We can improve these results by increasing the number of particles as shown in Figure 10. As the Reynolds number increases, the effect of the diffusion is less important and the discretization of the viscous term (7) with 400 particles, which works well at $Re = 1000$, is not fine enough to take into account this effect at higher Reynolds numbers; so this is balanced by increasing the number of particles.

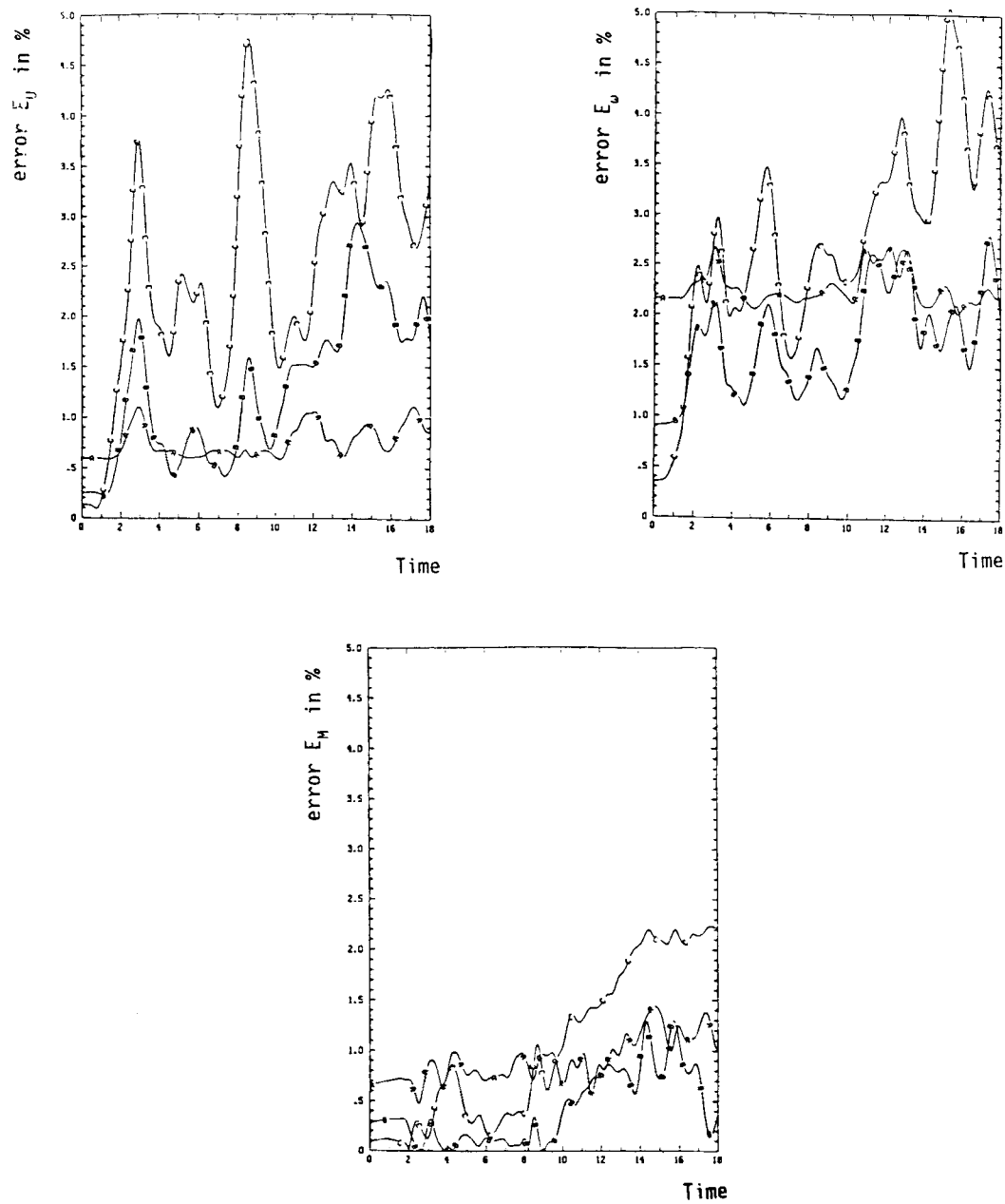

Figure 5. Influence of the cut-off parameter $\varepsilon = h^p$ for different values of p (A, 0·1, B, 0·2, C, 0·3); Navier–Stokes problem; regular case; $n_y = 5$; $\Delta t = 0{\cdot}03$; 400 particles; $Re = 10^4$

Although the error E_M is the only one available in the discontinuous case, we must remark that the results obtained do actually depend on the way of discretizing the functional $M(t)$. The quadrature formula necessary for its computation can be obtained either from the singular approximation ω^h of the vorticity defined by (4) or from its regularization defined by (15). We thus

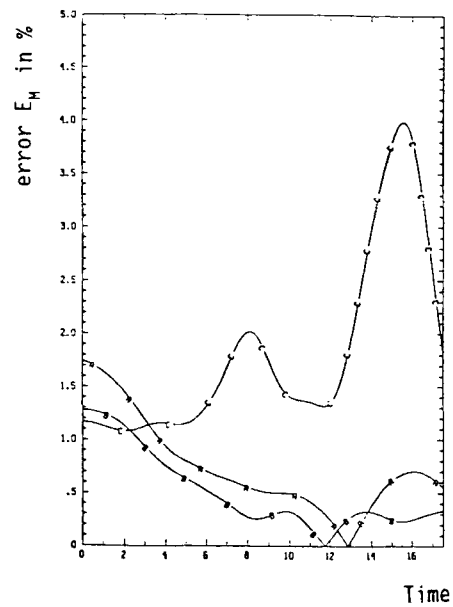

Figure 6. Influence of the cut-off parameter $\varepsilon = h^p$ for different values of p (A, 0·5; B, 0·6; C, 0·7); Navier–Stokes problem; discontinuous case; $n_\gamma = 2$; $\Delta t = 0{\cdot}05$; 400 particles; $Re = 10^3$

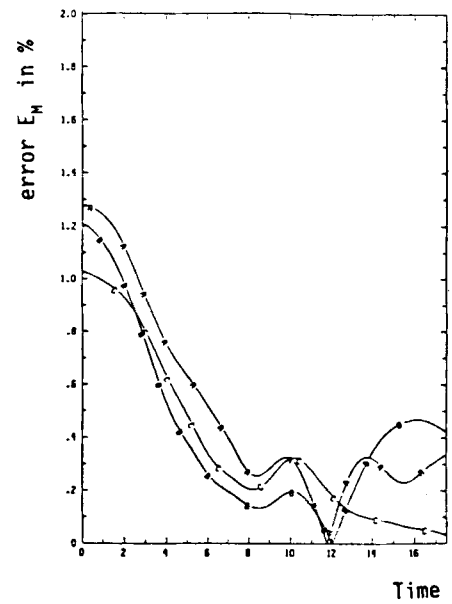

Figure 7. Influence of the number n_γ of internal iterations; (A, 2; B, 3; C, 5) Navier–Stokes problem; discontinuous case; $\varepsilon = h^{0{\cdot}5}$; $\Delta t = 0{\cdot}05$; 400 particles; $Re = 10^3$

obtain two other definitions:

$$M_h^{(2)}(t) = N_h^{(2)}(t)/D_h(t), \qquad N_h^{(2)}(t) = \sum_j \Omega_j(t)|z_j(t)|^2, \tag{25}$$

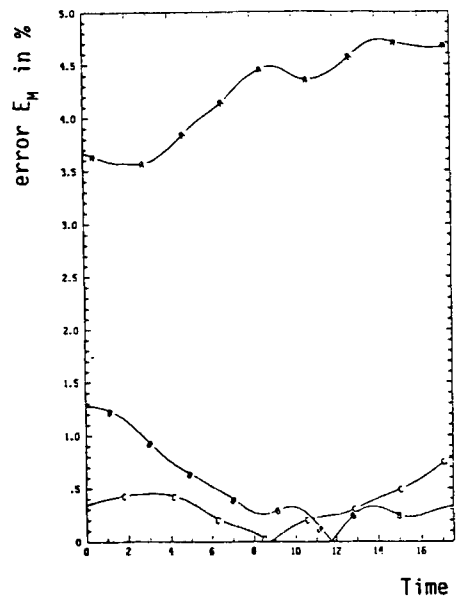

Figure 8. Influence of the number n_q (A, 225, B, 400; C, 625) of particles; Navier–Stokes problem; discontinuous case; $\varepsilon = h^{0.5}$; $n_\gamma = 2$; $\Delta t = 0.05$; $Re = 10^3$

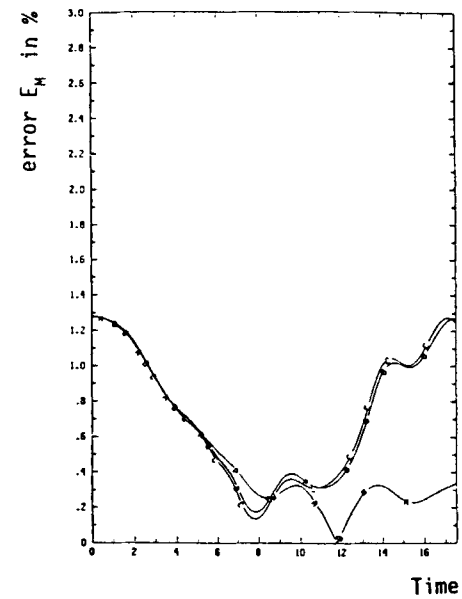

Figure 9. Influence of the Reynolds number (A, 10^3; B, 10^4; C, 10^5); Navier–Stokes problem; discontinuous case; $\varepsilon = h^{0.5}$; $n_\gamma = 2$; $\Delta t = 0.05$; 400 particles

$$M_h^{(3)}(t) = N_h(t)/D_h^{(3)}(t), \qquad D_h^{(3)}(t) = \sum_j h^2 \omega_h(z_j(t), t). \tag{26}$$

The scheme being conservative, the approximation $D_h(t)$ of the total vorticity is constant in time. Figure 11 presents the results obtained with the three definitions, in the regular case, and for

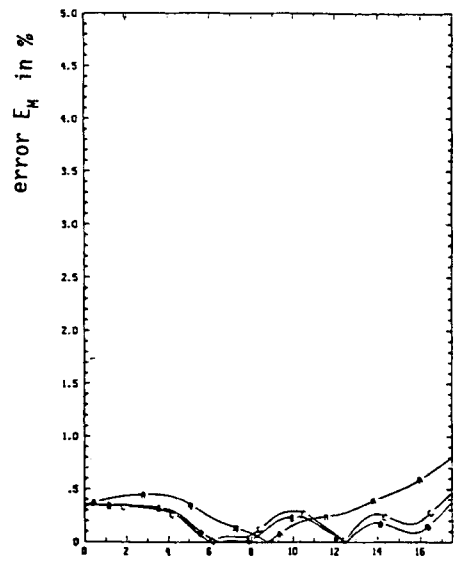

Figure 10. Influence of the Reynolds number (A, 10^3; B, 10^4; C, 10^5); Navier–Stokes problem; discontinuous case; $\varepsilon = h^{0.5}$; $n_\gamma = 2$; $\Delta t = 0.05$; 625 particles

Table II. 400 particles; $Re = 10^3$; $n_\gamma = 2$; $\Delta t = 0.05$; $\varepsilon = h^p$

p	0·2	0·4	0·5	0·6	0·7
$E_M(0)$	5·4	1·72	1·26	1·14	1·15
$E_M^{\max}$	5·45	1·72	1·26	1·14	3·98

different values of the number n_γ of internal iterations. We can first remark that definition (25), which is the one used by Roberts[2] for example, is the more favourable, with a maximum error during the time interval [0, 12] of order 0·1%, while our definition (22) gives an error of up to 27%. However, although the results are greatly dependent on the way of discretizing $M(t)$, the differences reduce considerably when using internal iterations, and the three definitions then give similar results.

The main aim of this paper has been to compare numerical solutions with analytical solutions. We want briefly to complete it by a comparison between our deterministic simulation of the diffusion and the previous random walk method proposed by Chorin.[1] We present by way of example two tests relative to the regular case defined by (24); they concern the accuracy of the methods in terms of the number of particles (Figure 12) and the influence of the Reynolds number (Figure 13).

In the random walk method the weight of each particle remains constant in time; on the other hand, each particle moves according to the law

$$z_j(t) = \tilde{z}_j(t) + \eta_j, \qquad \eta_j = (\eta_{jx}, \eta_{jy}),$$

where $\tilde{z}_j$ is determined by solving during Δt the classical convective part of the algorithm and where η_{jx} and η_{jy} are two Gaussian-distributed random variables with zero mean value and variance $\sigma^2 = 2\nu\Delta t$.

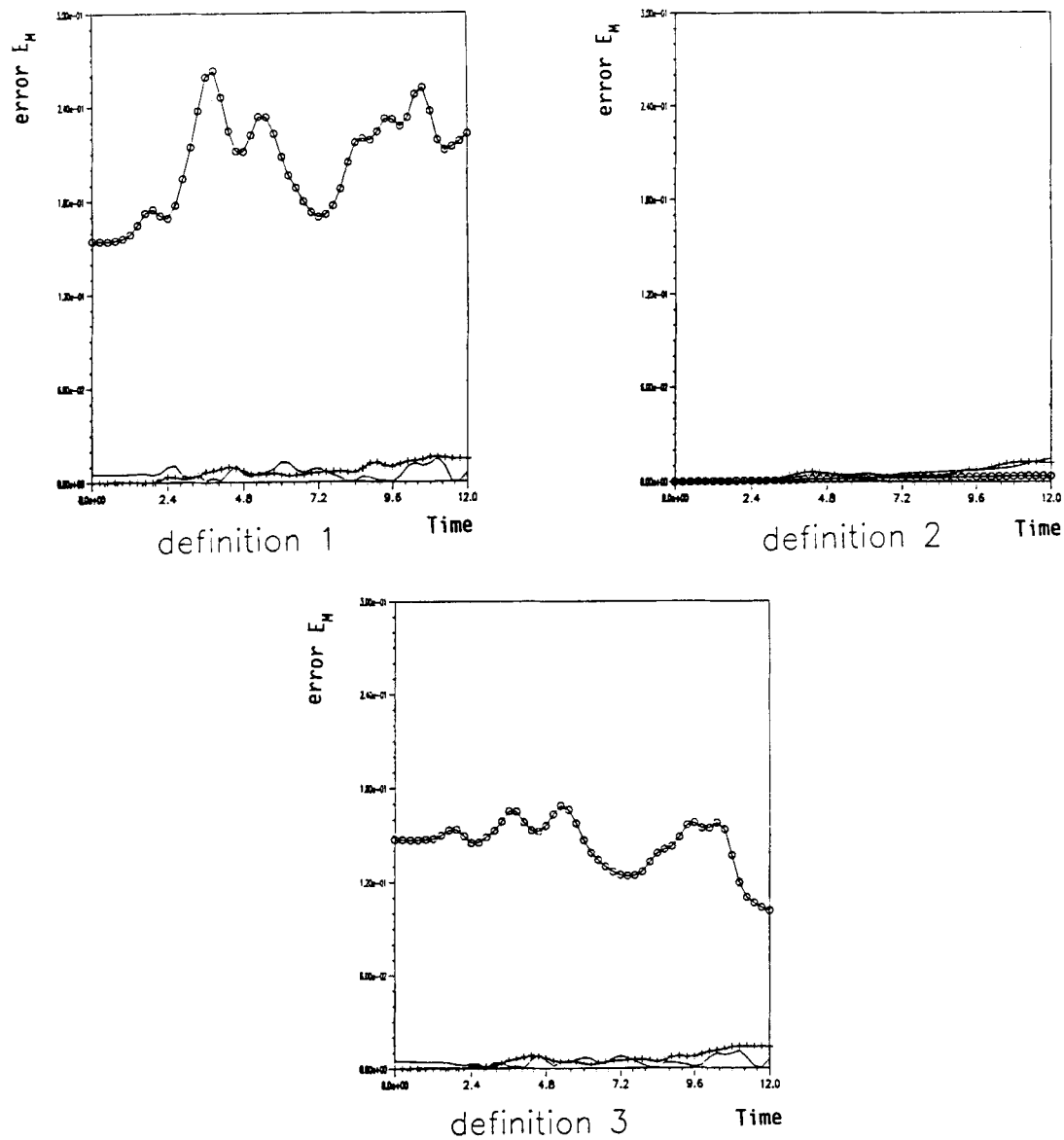

Figure 11. Influence of the definition of the moment error for different values of n_γ (⊖⊖, 0; ——, 2; + +, 5); regular case; $\varepsilon = h^{0.3}$; $\Delta t = 0.03$; 400 particles; $Re = 10^3$

Great care must be taken in the implementation of the random walk, as the results depend in practice on the way the Gaussian distribution is computed, and especially the random generator. Two initializations have been tested: a first from the NAG library and a second based on a classical congruence method. From a uniformly distributed sequence of points in [0, 1], the Gaussian distribution of points x has been constructed in three different ways: one from the NAG library, that of Roberts[2] and a third based on a polynomial approximation of the inverse of the cumulative distribution: t being a random number in the range $0 \leqslant t < 1$, the number x searched is $2^{1/2}\,\sigma\,\mathrm{erf}^{-1}(2t-1)$. Among these six simulations, five of them gave results that were nearly

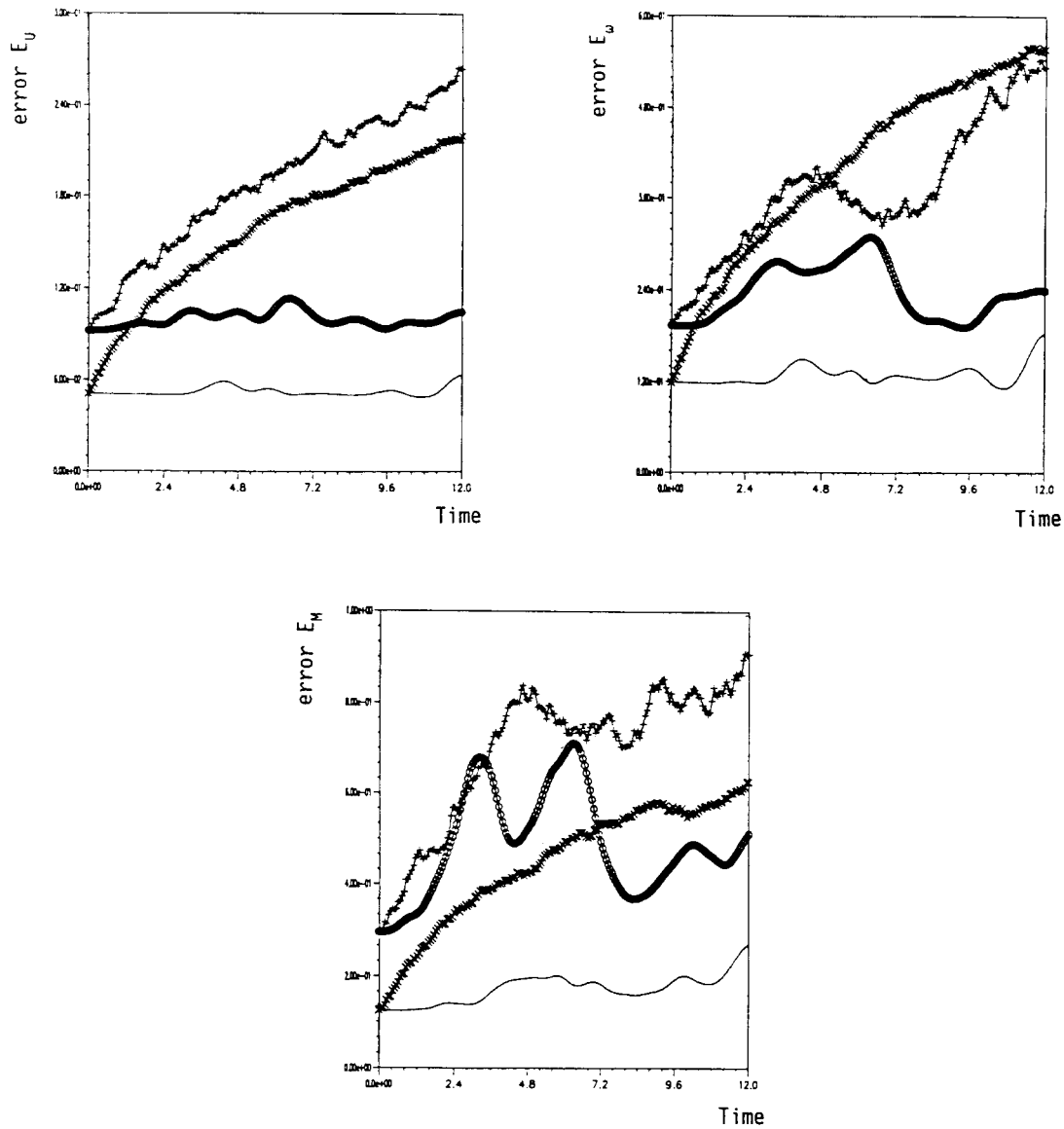

Figure 12. Comparison between the random walk method (+ +, $n_p = 100$; ×-×, $n_p = 625$) and our deterministic algorithm (o-o, $n_p = 100$; ——, $n_p = 625$) for different values of the number of particles; regular case; $\varepsilon = h^{0.3}$; $n_\gamma = 0$; $\Delta t = 0.03$; $Re = 10^3$

equivalent. The final choice was the one which gave the best result, that is the one using an approximation of the cumulative distribution and random numbers based on a congruence method.

Since in Chorin's method the weight of each particle remains constant in time, definition (25) of the moment can be simplified to

$$M_h^{(2)}(t) = \left(\sum_j |z_j(t)|^2 \right) \Big/ n_q,$$

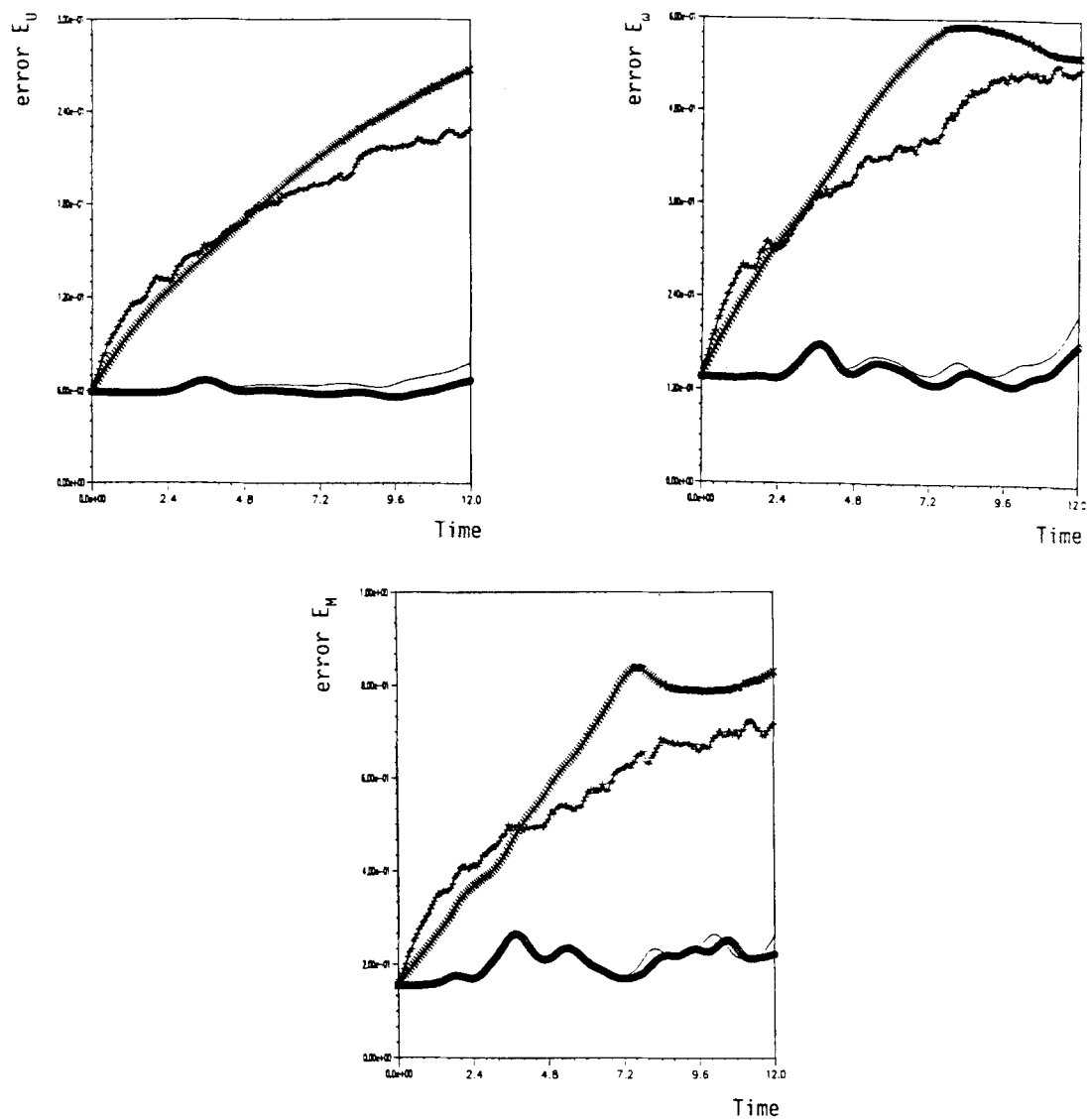

Figure 13. Comparison between the random walk method (+ +, $Re = 10^3$; ×-×, $Re = 10^5$) and our deterministic algorithm (o-o, $Re = 10^3$; ——, $Re = 10^5$) for different values of the Reynolds number; regular case; $\varepsilon = h^{0.3}$; $n_y = 0$; $\Delta t = 0.03$; 400 particles

where n_q is the number of particles. However, for a comparison with the deterministic algorithm, the first definition (22) has been kept, which explains, as seen above (see Figure 11), its important values. We have checked before that, with the second definition (25), the results we obtained in the singular case, according to our time scheme of order two, were of the same order of magnitude as that described by Roberts.[2]

Moreover, no internal iteration has been considered in this comparison, as this new method of interpolation of the vorticity function does not work in Chorin's method. This again explains the

large value of the errors, especially for the vorticity and the moment, as already seen for the case in Figure 3.

The theoretical results show that the rate of convergence of the random method is of order $\nu^{1/2}/n_q^{1/2}$. This is consistent with the numerical results presented in Figures 12 and 13, where Chorin's method seems to be less accurate and more sensitive to variation of the Reynolds number. Let us however emphasize that the algorithm (6), (7) is more expensive than the random walk, the ratio of cost being 1·6 for 400 particles (0·028 CPU time per time step for the deterministic algorithm).

In all these computations we can remark that the initial errors are different from zero; this is due to the fact that we do not use the exact value of the initial data, unlike in the case of classical methods such as finite difference methods.

CONCLUSIONS

The importance of the choice of the cut-off parameter ε in the particle method has been pointed out. According to the theoretical results, in the particular case of the splitting algorithm,[4] or in the linear case,[8] this parameter is greater here than in the inviscid case. We have also shown the necessity of a good interpolation of the vorticity function, as was already the case for the Euler equations.[13] However, the important increase in the computational cost as a function of the number n_γ of internal iterations (20% CPU for $n_\gamma = 2$, 50% CPU for $n_\gamma = 5$) and the improvement of the accuracy thus involved do not justify the use of a large number n_γ of internal iterations.

We have also noted that it does not seem necessary to use a large number of particles. Over a certain value (225 particles for the first example and 400 for the second), the results obtained are similar. As for the finite difference method, high Reynolds computations require an increase in the number of points of discretization (here particles). Finally, this method seems to be easier to use than the splitting one, where a main difficulty is the choice of the splitting time step.[7]

As for the case of vortex methods for inviscid fluids[16] and for the random walk method for viscous fluids,[2] the algorithm described in the present paper is adapted to non-smooth initial data.

ACKNOWLEDGEMENT

The computational cost was supported financially by the CCVR.

APPENDIX

Let us recall in 2D the proof of the following consistency result: $I_\alpha = 1$ if $\alpha = (2, 0)$ or $(0, 2)$ and $I_\alpha = 0$ otherwise. By definition,

$$I_\alpha = \int_{\mathbb{R}^2} (z' - z)^\alpha \frac{D\zeta_\varepsilon(z - z')\cdot(z' - z)}{\|z - z'\|^2} \mathrm{d}z'.$$

As assumed previously, ζ is of radial symmetry and is an approximation of order k of δ, so that $\zeta(z) = \bar{\zeta}(|z|)$ and

$$\int_0^\infty \rho\bar{\zeta}(\rho)\,\mathrm{d}\rho = 1/2\pi, \tag{27}$$

$$\int_0^\infty \rho^{l+1}\bar{\zeta}(\rho)\,\mathrm{d}\rho = 0, \quad l = 1, \ldots, k-1, \quad l \text{ even}, \tag{28}$$

$$\int_0^\infty \rho^{k+1}|\bar{\zeta}(\rho)|\,\mathrm{d}\rho < \infty. \tag{29}$$

Setting $\zeta_\varepsilon(z) = (1/\varepsilon^2)\zeta(z/\varepsilon)$, we have

$$D\zeta_\varepsilon(z)\cdot z = (|z|/\varepsilon^3)\bar{\zeta}'(|z|/\varepsilon).$$

Finally, setting $z'-z=\varepsilon\rho\Omega$, with Ω in S_1 (the unit sphere in $\mathbb{R}^2$), the previous integral can be written as:

$$I_\alpha = -\varepsilon^{|\alpha|-2}\left(\int_0^\infty \rho^{|\alpha|}\bar{\zeta}'(\rho)\,d\rho\right)\cdot J_\alpha,$$

with

$$J_\alpha = \int_{S_1} \Omega^\alpha\, d\Omega.$$

Using the fact that: $1 \leqslant |\alpha| \leqslant k+1$ and inequality (29), we deduce:

$$\lim_{\rho\to 0} \rho^{|\alpha|}\bar{\zeta}(\rho) = \lim_{\rho\to\infty} \rho^{|\alpha|}\bar{\zeta}(\rho) = 0.$$

Integration by parts then gives

$$I_\alpha = \varepsilon^{|\alpha|-2}|\alpha|\left(\int_0^\infty \rho^{|\alpha|-1}\bar{\zeta}(\rho)\,d\rho\right)\cdot J_\alpha.$$

We remark that $J_\alpha = 0$ if one of the coefficients α_i is odd, and by (28) the integral above is equal to 0 for $|\alpha|$ even and $4 \leqslant |\alpha| \leqslant k+1$. Thus the only two cases for which $I_\alpha \neq 0$ are $\alpha = (2, 0)$ or $(0, 2)$; one easily verifies that the resulting value of I_α is then equal to 1.

REFERENCES

1. A. J. Chorin, 'Numerical study of slightly viscous flow', *J. Fluid Mech.*, **57,** 785 (1973).
2. S. Roberts, 'Accuracy of the random walk method for a problem with a non smooth initial data', *J. Comput. Phys.*, **58,** 29 (1985).
3. P. R. Spalart, 'Numerical simulation of separated flows', *NASA Technical Memorandum 84328*, 1984.
4. G. H. Cottet and S. Gallic, 'A particle method to solve transport diffusion equations, part II: The non linear case', *Rapport Interne No. 158*, Centre de Mathématiques Appliquées de l'Ecole Polytechnique Palaiseau, April 1987.
5. S. Huberson, 'Modélisation asymptotique et numérique de noyaux tourbillonnaires enroulés', *Thèse d'etat*, Université Pierre et Marie Curie, Paris, 1986.
6. J. P. Choquin and S. Huberson, 'Application de la méthode particulaire aux écoulements à grand nombre de Reynolds', 18*ème Congrès National d'Analyse* Numérique, Puy St Vincent, 20–24 May 1985.
7. B. Lucquin-Desreux, 'Approximation particulaire des équations de Navier–Stokes bidimensionnelles', *La Recherche Aérospatiale*, **4,** 1–12 (1987).
8. S. Mas-Gallic and P. A. Raviart, 'Particle approximation of convection diffusion problems', *Publication No. R86013*, Laboratoire d'Analyse Numérique de l'Université Pierre et Marie Curie, Paris, 1986.
9. P. A. Raviart, 'An analysis of particle methods', *CIME Course, Numerical Methods in Fluid Dynamics*, Como, July 1983.
10. O. Hald, 'The convergence of vortex method II', *SIAM J. Numer. Anal.*, **16,** 726 (1979).
11. J. T. Beale and A. Majda, 'High order accurate vortex methods with explicit velocity kernel', *J. Comput. Phys.*, **58,** 188 (1985).
12. R. A. Nicolaides, 'Construction of higher order accurate vortex and particles methods', *Appl. Numer. Math.*, **2,** 313 (1986).
13. J. T. Beale, 'On the accuracy of vortex methods at large times', *Proc. Workshop on Computational Fluids Dynamics and Reacting Gas Flows*, Institute of Applied Mathematics, Mineapolis, September 1986.
14. R. Franke, 'Scattered data interpolation', *Math. Comput.*, **38,** 181 (1982).
15. F. Milinazzo and P. G. Saffman, 'The calculation of large Reynolds number two dimensional flows using discrete vortices with a random walk', *J. Comput. Phys.*, **23,** 380 (1977).
16. M. Perlman, 'On the accuracy of vortex methods', *J. Comput. Phys.*, **59,** 200 (1985).